bonate + *n*-decane, *n*-dodecane, *n*-tetradecane, and *n*-hexadecane, respectively. The value found in the literature is $\delta_1 = 20\ J^{1/2}\ cm^{-3/2}$ (*6*).

Glossary

a	coefficients in eq 1
x	mole fraction
H	molar enthalpy, J mol^{-1}
T	temperature, K
R	molar gas constant, J K^{-1} mol^{-1}
V	molar volume, m^3 mol^{-1}

Greek Letters

δ	solubility parameter, J$^{1/2}$ cm$^{-3/2}$
Φ	volume fraction, $\Phi_i = x_iV_i/(x_1V_1 + x_2V_2)$ (i = 1, 2)
σ	standard deviation, eq 2

Subscripts

i	property of component i (i = 1, 2)

Superscripts

E	excess property
c	critical point property

Literature Cited

(1) Kehiaian, H. V. *Pure Appl. Chem.* **1985**, *57*, 15.
(2) Garcia, I.; Cobos, J. C.; Gonzalez, J. A.; Casanova, C.; Cocero, M. J. *J. Chem. Eng. Data* **1988**, *33*, 423.
(3) Garcia, I.; Cobos, J. C.; Gonzalez, J. A.; Casanova, C. *Int. DATA Ser., Sel. Data Mixtures, Ser A* **1987**, 164–173.
(4) Cocero, M. J.; Mato, F.; Garcia, I.; Cobos, J. C.; Kehiaian, H. V. *J. Chem. Eng. Data* **1989**, *34*, 73.
(5) Cocero, M. J.; Mato, F.; Garcia, I.; Cobos, J. C. *J. Chem. Eng. Data* **1989**, *34*, 443.
(6) *CRC Handbook of Chemistry and Physics*, 69th ed.; CRC Press: West Palm Beach, FL, 1989; pp C-197, C-681.
(7) Riddick, J. A.; Bunger, W. B.; Sakano, T. K. *Organic Solvents: Physical Properties and Methods of Purification*; Wiley: New York, 1986; Vol. II, pp 129, 132.
(8) TRC Thermodynamics Tables—Hydrocarbons; Thermodynamics Research Center, The Texas A&M University System: College Station TX, 1986; pp aa-1650, aa-1670, m-1012.
(9) Gopal, R.; Rice, O. K. *J. Chem. Phys.* **1955**, *23*, 2428.
(10) Loven, A. W.; Rice, O. K. *Trans. Faraday Soc.* **1963**, *59*, 2723.
(11) Young, C. L. *Trans. Faraday Soc.* **1969**, *65*, 2639.
(12) Snyder, R. B.; Eckert, C. A. *J. Chem. Eng. Data* **1973**, *18*, 282.
(13) Balasubramanian D.; Mitra, P. *J. Phys. Chem.* **1979**, *83*, 2724.
(14) Tveekrem, J. L.; Jacobs, D. T. *Phys. Rev. A* **1983**, *27*, 2773.
(15) Cohn, R. H.; Jacobs, D. T. *J. Chem. Phys.* **1984**, *80*, 856.
(16) Hildebrand, J. H.; Scott, R. L. *Regular Solutions*; International Series in Chemistry; Prentice Hall: Englewood Cliffs, NJ, 1962.
(17) Majer, V.; Svoboda, V. *Enthalpies of Vaporization of Organic Compounds*; Blackwell: Oxford, U.K., 1985.

Received for review March 29, 1990. Revised August 24, 1990. Accepted November 25, 1990.

Transport Properties in the Molten Binary System $CH_3NH_3Cl–C_2H_5NH_3Cl$

Grazyna Zabinska, Grazyna Urbaniak, and Adolf Kisza
Institute of Chemistry, University of Wroclaw, Ul. F. Joliot-Curie, 14, 50383 Wroclaw, Poland

Paolo L. Ferloni*
Dipartimento di Chimica fisica della Universitá and CSTE-CNR, Viale Taramelli, 16, 27100 Pavia, Italy

As the simplest case in a series of molten binary systems containing alkylammonium chlorides, the system $CH_3NH_3Cl–C_2H_5NH_3Cl$ [(MA)Cl–(EA)Cl] was investigated. The liquidus curve is of the simple eutectic type, with $T_e = 347 \pm 3$ K and eutectic composition of 0.710 in ethylammonium chloride. Densities, conductivities, and viscosities of molten mixtures were measured in the whole composition range, for $0 < x_2 < 1$. From the results obtained, one can conclude that the behavior of the system is not ideal. Owing to its interesting transport properties, the eutectic mixture can be proposed as a convenient molten electrolyte above 353 K.

Introduction

In a series of previous papers, the transport properties of binary molten mixtures formed with alkylammonium halides (*1*, *2*) and sodium and potassium acetates (*3*) were investigated. The interest of these works lays in the fact that salts formed with organic ions, alkylammonium in particular, can find wide application in electrochemistry, not only as supporting electrolytes in nonaqueous solvent systems but also in several electrochemical methods of analytical and industrial importance.

However, with physicochemical information about this class of molten systems being still fragmentary [see, e.g., a recent review (*4*)], it seemed worthy to extend the investigation to further systems containing alkylammonium chlorides. It is well-known that the formation of a binary mixture of salts with organic ions usually involves changes in molar volumes, conductivities, and viscosities. The determination of these properties could allow one to evaluate the influence of ion size, acid–base characteristics, and intermolecular interactions on the structure of the melts in the mixture.

In this paper, the molar volumes, conductivities, and viscosities of nine mixtures in one of the simplest systems of this type, viz., the binary formed with CH_3NH_3Cl [(MA)Cl] and $C_2H_5NH_3Cl$ [(EA)Cl], are reported and discussed in connection with the phase diagram of the system.

Experimental Section

Materials. The salts were obtained by neutralization of the amines (both Fluka, purum) with HCl (Polskie Odczynniki Chemiczne (P.O.Ch.), Gliwice, Poland; czysty). After evaporation of the aqueous solutions, the salts were recrystallized at least twice from ethanol (P.O.Ch.; absolutny); their melting point was checked by microscopic observation with a Boetius type apparatus. The pure salts, as well as the binary mixtures, prepared by melting the preweighed components under nitrogen, were stored under vacuum before measurements.

The salts employed for determining the phase diagram were reagent grade chemicals supplied by Aldrich. They were kept in a vacuum oven for 48 h at ~80 °C before use.

0021-9568/91/1736-0164$02.50/0

Table I. Experimental Densities (ρ_{12}) of Molten (MA)Cl (x_1)-(EA)Cl (x_2) Mixtures at Several Temperatures

	$\rho_{12} \pm 5 \times 10^{-4}$, g cm^{-3}										
T, K	$x_2 = 0$	$x_2 = 0.1$	$x_2 = 0.2$	$x_2 = 0.3$	$x_2 = 0.4$	$x_2 = 0.5$	$x_2 = 0.6$	$x_2 = 0.7$	$x_2 = 0.8$	$x_2 = 0.9$	$x_2 = 1.0$
413											0.9965
423						1.0268	1.0343		1.0135	1.0082	0.9921
433					1.0344	1.0218	1.0279		1.0082	1.0029	0.9878
443					1.0293	1.0168	1.0217	1.0087	1.0029	0.9976	0.9834
453				1.0324	1.0243	1.0119	1.0160	1.0032	0.9987	0.9925	0.9791
463				1.0252	1.0193	1.0070	1.0110	0.9981	0.9935	0.9874	0.9747
473			1.0395	1.0204	1.0143	1.0022	1.0064	0.9941	0.9894	0.9823	0.9704
483			1.0342	1.0157	1.0119	0.9974	1.0014	0.9914	0.9858	0.9773	0.9661
493		1.0306	1.0290	1.0110	1.0070		0.9975	0.9874	0.9813	0.9723	0.9617
503	1.0264	1.0253	1.0238	1.0064	1.0022		0.9926	0.9829	0.9773		0.9574
513	1.0207	1.0202	1.0187			0.9875	0.9877				
523	1.0150	1.0150									
533	1.0093										

***Transport Measurements*.** Electrical conductivity, viscosity, and density were measured between 393 and 543 K on the pure components and nine mixtures of composition $0.1 < x_2 < 0.9$, component 2 being ethylammonium chloride; for each measurement, 20-60 g of substance were employed.

For conductivity, an H type cell with Pt electrodes was used. The cell constant was determined by means of a standard solution of KCl in water at 25 °C and was found to be 22.84 ± 0.05 cm^{-1}. Conductivities were measured with an automatic C bridge type E 315 A (Meratronik, Szczecin, Poland) at 1 kHz; the precision of the conductance measurements was about 0.1%.

Viscosity was determined with a modified Ostwald type viscosimeter, described earlier (*3*). The flow of the liquid volume through a glass capillary was measured with an electronic quartz clock with an accuracy of ±0.015 in the range of 100 s. The viscosimeter was calibrated by using ethylammonium chloride, the viscosity of which had been previously determined in our laboratory (*5*).

Density was determined by a pycnometric method with fused ethylammonium chloride as standard (*6*).

The standard deviations of the conductivity, viscosity, and density data were $\pm 5 \times 10^{-4}$ S cm^{-1}, $\pm 5 \times 10^{-6}$ Pa s, and $\pm 5 \times 10^{-4}$ g cm^{-3}, respectively.

***Phase Diagram Determination*.** The phase diagram was determined by means of both visual polythermal analysis and differential scanning calorimetry (dsc) with a Perkin-Elmer DSC-2. Mixtures weighing 0.7-1.3 g were sealed under vacuum in Pyrex tubes and submitted to repeated cycles of fusion and crystallization. The liquidus curve was determined by visual observation of crystals formed on cooling the molten mixtures under vigorous stirring. Temperatures were measured with a chromel-alumel thermocouple connected with a Leeds & Northrup type 8690-2 millivolt potentiometer. After this treatment, the tubes were opened, the mixtures were thoroughly ground, and samples weighing 3-6 mg were sealed in Al pans. In order to avoid possible decomposition due to the oxygen sealed in the pan, just before each dsc scan, a hole was drilled into the pan cover, thus allowing dry nitrogen to flow over the sample during the measurements. The instrument was calibrated as previously reported (*7*). The investigated temperature range was from 320 K to some degrees above fusion. The precision in T measurements was ±1 K.

Results

The (MA)Cl and (EA)Cl used as components for the phase diagram melted at 502 ± 1 and 384 ± 2 K, with heats of fusion 13 ± 1 and 6 ± 1 kJ mol^{-1}, respectively. A solid-solid-phase transition was found in component 2 [(EA)Cl] at 355 ± 3 K, with a latent heat of 11 ± 1 kJ mol^{-1}.

The phase diagram of this binary system is presented in Figure 1. From the liquidus curve, as determined by visual observation and confirmed by dsc measurements, the system is of the simple eutectic type, with eutectic temperature T_e = 347 ± 3 K and composition $x_{2,e}$ = 0.710. It can be remarked that the solid-solid transition observed at 355 K in (EA)Cl is just a few degrees above the eutectic temperature.

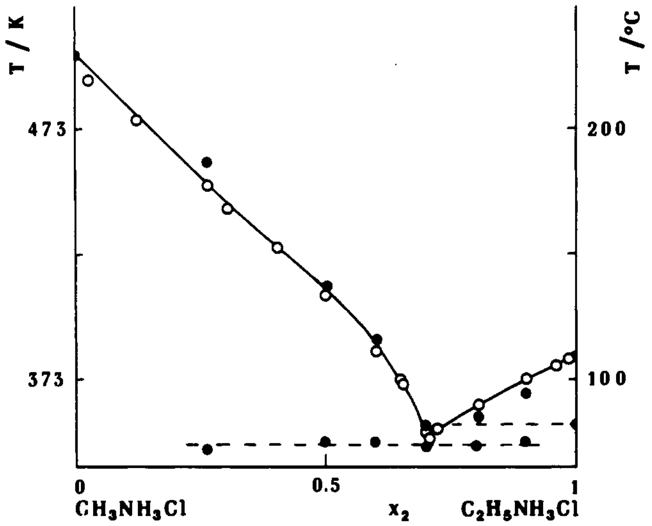

Figure 1. Phase diagram of the system CH_3NH_3Cl-$C_2H_5NH_3Cl$: (○) visual observation; (●) dsc data.

The density, electrical conductivity, and viscosity data, collected at different temperatures for the pure salts and for the investigated mixtures, are presented in Tables I-III. The data for the pure components are practically coincident with those previously published (*4*).

Discussion

The thermal behavior of the salts forming the present system was previously investigated with dsc by Tsau and Gilson (*8*), who found that (MA)Cl melts with sublimation at 506 K, and (EA)Cl melts at 381 K with a fusion heat of 9.8 kJ mol^{-1}; no transitions were observed by them in the latter salt. The present melting points are in agreement with those of Tsau and Gilson, whereas the heat of fusion we found for (EA)Cl is substantially lower. Owing to sublimation, the present heat of fusion for pure (MA)Cl should be considered as a tentative and provisional value. On the other side, the solid-solid transition brought out on (EA)Cl seems to be in agreement with the higher transition found on this salt by means of IR spectroscopy by Rao et al. (*9*) at 345 K with a heat of transition of 7.4 kJ mol^{-1}, i.e. a value significantly lower than the present one. Other solid-solid-phase transitions, reported in the literature for both salts (*8*, *9*) and occurring at temperatures lower than T_e, are not relevant to the present work.

As for the molten mixtures, the nonideal character of the system can be tested by plotting the molar properties of the

Table II. Experimental Viscosities (η_{12}) of Molten (MA)Cl (x_1) + (EA)Cl (x_2) Mixtures at Several Temperatures

	($\eta_{12} \times 10^3$) ■ (5×10^{-6}), Pa s										
T, K	$x_2 = 0$	$x_2 = 0.1$	$x_2 = 0.2$	$x_2 = 0.3$	$x_2 = 0.4$	$x_2 = 0.5$	$x_2 = 0.6$	$x_2 = 0.7$	$x_2 = 0.8$	$x_2 = 0.9$	$x_2 = 1.0$
393											16.048
403											13.269
413											10.854
423											9.260
433										6.398	7.988
438						4.551	4.866	6.213	6.449	5.804	
443					3.408	4.254	4.346	5.724	5.784	5.279	6.738
448					3.068	3.850	3.940	5.225	5.356	4.857	
453				2.512	2.735	3.521	3.641	4.737	4.864	4.418	5.940
458				2.153	2.431	3.200	3.255	4.284	4.462	4.042	
463				2.022	2.173	2.815	2.933	3.943	4.078	3.719	5.234
468				1.741	1.878	2.575	2.645	3.574	3.814	3.368	
473			1.362	1.542	1.658	2.320	2.385	3.337	3.459	3.107	4.613
478			0.995	1.334	1.447	2.091		2.980	3.185	2.935	
483			0.824								4.275
488			0.755								
493		0.539	0.649								3.884
498			0.612								
503	2.438	0.441									
508	2.340										
513	2.259	0.380									
518	2.155										
523	2.085	0.344									
533	1.961										

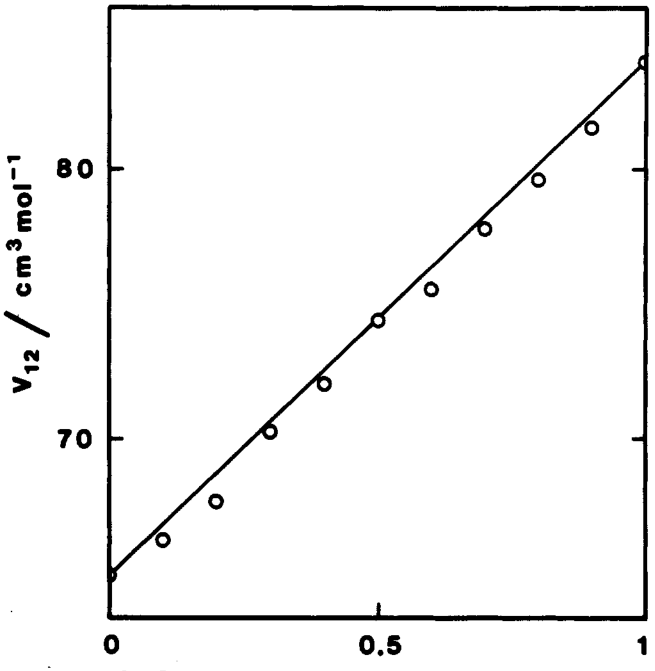

Figure 2. Molar volume versus the mole fraction of (EA)Cl at 473 K. The data for $x_2 = 0$ and 0.1 were obtained by extrapolation. Solid line: ideal behavior.

mixtures as a function of the mole fraction of the solute [(EA)Cl, x_2].

The molar volume, V_{12}, is given by the ratio

$$V_{12} = M_{12}/\rho_{12} \tag{1}$$

where $M_{12} = x_1M_1 + x_2M_2$ is the mean molar mass of the mixture, M_1 and M_2 being the molar masses of (MA)Cl and (EA)Cl, respectively, and ρ_{12} is the density of the mixture.

Figure 2 presents the plot of the molar volume vs the mole fraction of (EA)Cl at 473 K. In the whole composition range, the actual molar volume of the molten mixtures is lower than the straight line calculated for the ideal mixtures. In pure molten alkylammonium chlorides, the Coulombic interactions of the alkylammonium cation with the surrounding chloride anions are equal. In the considered molten mixtures, the Coulombic interactions of the smaller MA$^+$ cations are stronger than those of the larger EA$^+$ one. As a result of this situation, the chloride anion should shift toward the MA$^+$ cation, to a distance, on the average, shorter than that in pure molten (MA)Cl. On a macroscopic scale, this obviously leads to the volume contraction observed as a negative deviation of the molar volume from the ideal behavior.

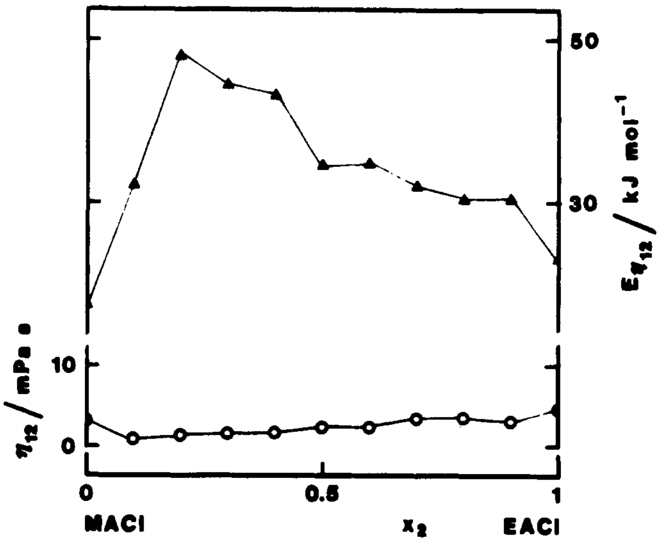

Figure 3. Viscosity (○) and activation energy for viscous flow (▲) at 473 K. The data for $x_2 = 0$ and 0.1 were obtained by extrapolation.

Such views can be confirmed by the results of viscosity measurements: In Figure 3, viscosities and their activation energies are given, as an example, at 473 K.

One can also see that for intermediate compositions the activation energy of the viscous flow is much higher than those for compositions close to the pure components. The activation energy of the viscous flow, as calculated from the Arrhenius type equation

$$\eta_{12} = \eta_{12}^{\infty} \exp(E_{\eta_{12}}/RT) \tag{2}$$

appears to be a temperature-dependent quantity in this molten binary system. A similar behavior was observed in molten ammonium picrates (*10*). The experimental viscosities are slightly lower than the additive values (ideal viscosities). This

Table III. Experimental Conductivities (κ_{12}) of Molten (MA)Cl (x_1) + (EA)Cl (x_2) Mixtures at Several Temperatures

	$\kappa_{12} \pm 5 \times 10^{-4}\ \Omega^{-1}\ \mathrm{cm}^{-1}$										
T, K	$x_2 = 0$	$x_2 = 0.1$	$x_2 = 0.2$	$x_2 = 0.3$	$x_2 = 0.4$	$x_2 = 0.5$	$x_2 = 0.6$	$x_2 = 0.7$	$x_2 = 0.8$	$x_2 = 0.9$	$x_2 = 1.0$
393											0.0648
413											0.0864
423								0.1486	0.1371	0.1271	
428							0.1690	0.1573	0.1461	0.1335	
433						0.1971	0.1822	0.1658	0.1549	0.1409	0.1098
438					0.2371	0.2080	0.1920	0.1746	0.1633	0.1481	
443					0.2499	0.2185	0.2018	0.1833	0.1722	0.1547	
448					0.2613	0.2298	0.2125	0.1929	0.1803	0.1604	
453				0.2903	0.2734	0.2406	0.2228	0.2023	0.1899	0.1656	0.1352
458				0.3036	0.2856	0.2524	0.2335	0.2116	0.1990	0.1746	
463				0.3157	0.2974	0.2636	0.2437	0.2198	0.2080	0.1800	
468				0.3287	0.3084	0.2748	0.2542	0.2298	0.2172	0.1862	
473			0.3454	0.3408	0.3184	0.2858	0.2648	0.2387	0.2261		0.1625
478			0.3596	0.3536							
483			0.3724	0.3653							
488		0.3888	0.3852								
493		0.3995									0.1916
498		0.4101									
503	0.4526										
513	0.4789										
523	0.5038										
533	0.5274										

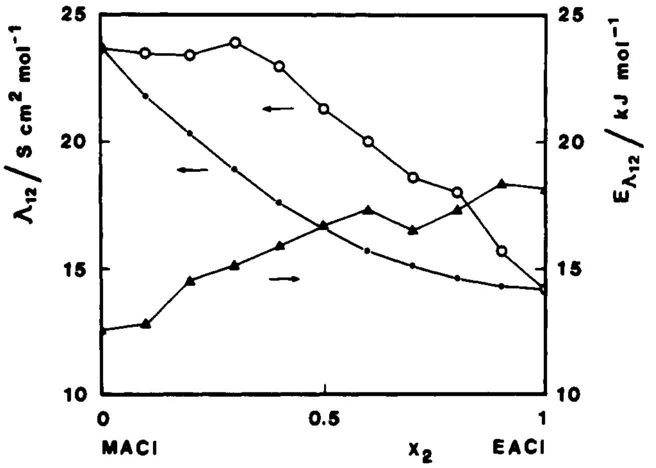

Figure 4. Electrical conductivity (○) and activation energy for electrical conductivity (▲) at 473 K: (-●-) values calculated by means of Markov and Sumina's equation. The data for $x_2 = 0$ and 0.1 were obtained by extrapolation; the datum for $x_2 = 0.9$ was taken from ref 6.

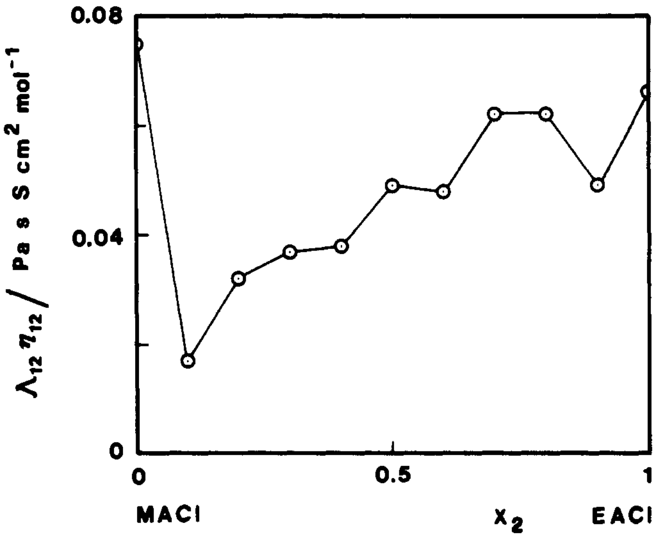

Figure 5. Plot of the Walden product, $\lambda_{12}\eta_{12}$, versus the mole fraction of (EA)Cl at 473 K.

indicates that the momentum transfer in the mixtures is facilitated in comparison with those of the pure molten components. Such change in the "fragility" of the liquid was also observed in molten solutions of metal chlorides in α-picolinium chloride (*11*, *12*).

The plot of the molar conductance as a function of composition at 473 K is shown in Figure 4, together with the values calculated from Markov-Sumina's equation (*13*, *14*), showing negative deviations from simple additivity. The trend of the corresponding activation energy is also illustrated. In the case of conductance, the activation energy can be evaluated from the Arrhenius type equation

$$\lambda_{12} = \lambda_{12}^{\infty} \exp\left(-\frac{E_{\lambda_{12}}}{RT}\right) \qquad (3)$$

but again it appears to be a temperature dependent quantity.

One can remark that the behavior of conductance is different from that of viscosity. The experimental molar conductances are higher than those of the ideal mixtures and decrease systematically with increasing content of (EA)Cl, owing to the greater influence of the larger size of the EA$^+$ cation and to the consequent change in the Coulombic interaction. The activation energy of the conductance process, however, shows random deviations (both positive and negative) from simple additivity. Such behavior is different from that of the activation energy of viscous flow, which shows only positive deviations in the whole concentration range (Figure 3). A possible explanation of this difference can be found by supposing that the ionic species mainly involved in the momentum transfer are not coincident with those responsible for the transport of charge. In fact, the hydrogen cations present in these melts as a result of the acidic dissociation of the alkylammonium ions may contribute significantly to the transport of electrical charge, while giving only a minor contribution to the viscous flow in the mixture.

This may also be the reason why the Walden product $\lambda_{12}\cdot\eta_{12}$ (*15*) is significantly dependent on temperature and concentration (Figure 5).

As it was shown in the above discussion, the transport properties of these molten organic salts and their mixtures cannot be adequately described by the Arrhenius type equation as derived from the simple Eyring's rate theory (*16*).

Several equations have been proposed (*4*) to account for the non-Arrhenius behavior of liquids. Angell (*17*–*20*), Easteal and Hodge (*21*), and Bloom and Macky (*22*) have thoroughly discussed the transport properties of molten binary mixtures in terms of free volume theories of liquids. The equations relating

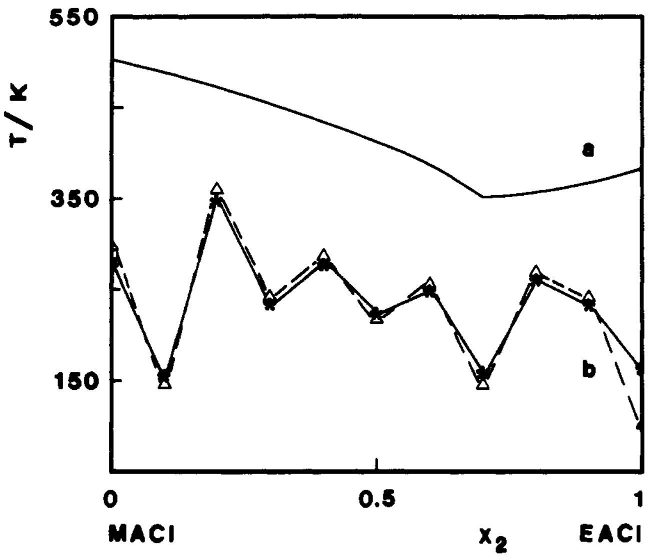

Figure 6. Liquidus curve of the (MA)Cl–(EA)Cl system (a) and T_0 values (b) calculated from eqs 4 (✱) and 5 (△).

transport properties, e.g. molar conductance, to temperature differ from the simple Arrhenius type equation by the incorporation of the temperature T_0. After Cohen and Turnbull (*23*), this temperature is related to the glass-transition temperature T_g by the relationship $T_0 < T_g$. The three-parameter VTF equation reads

$$\lambda_{12} = A \exp\left(-\frac{B}{T - T_0}\right) \tag{4}$$

where A, B, and T_0 are constants.

In the theory developed by Adams and Gibbs (*24*), diffusion in the melt takes place by cooperative rearrangements of groups of ions, and in their model, configurational entropy replaces free volume. As the temperature decreases, the number of configurations available to the system decreases, giving only one configuration at T_0. These authors derived the following equation:

$$\lambda_{12} = A' \exp\left(-\frac{B'}{T \ln (T/T_0)}\right) \tag{5}$$

Both eqs 4 and 5 have been used to fit the experimental data of conductivity in order to evaluate the T_0 temperature as a function of composition in the present system. The results of these fittings are presented in Figure 6, together with the liquidus line of the phase diagram.

Although the evaluation of T_0 is very sensitive to the accuracy of the experimental data, it seems surprising that the fittings according to both mentioned equations give almost the same results. This might suggest that on the basis of the available data it is not possible to differentiate one model from another.

Concluding Remarks

The general conclusion drawn from the present results is that the behavior of the (MA)Cl + (EA)Cl molten mixtures is not ideal. A first clue to this interpretation is given by the phase diagram in Figure 1. Although there is no evidence of any definite formation of an intermediate compound, this type of binary phase diagram is formed between components showing appreciable differences in the sizes of their cations and in the resulting ionic potentials (*25*). In the present case, the two cations have different sizes: the calculated radii of MA^+ and EA^+ being 1.136×10^{-10} m and 1.278×10^{-10} m, respectively (*26*); the Coulombic interactions are not equal.

Another contribution to the intermolecular interactions in this molten system is given by the acid–base properties of the alkylammonium cations (*27*). The existence of H^+ ions resulting from the acidic dissociation of both alkylammonium cations may lead to the formation of weak hydrogen bonds. Binary mixtures with such specific interactions usually exhibit deviations from the ideal behavior. The maximum conductivity for $x_2 = 0.30$ seems to be associated with stronger acid properties of methylammonium chloride and possibly increased formation of H bonds within the melts for compositions $0.2 < x_2 < 0.4$.

As for viscosity, which is more sensitive to structural changes in the mixing process, the deviation from ideality reaches a minimum for $x_2 = 0.80$, i.e., as expected, near the eutectic region of the phase diagram.

Finally, it can be noticed that the eutectic mixture with $x_2 = 0.710$, owing to its interesting transport properties, can be proposed as a suitable molten electrolyte above 353 K.

Registry No. $MeNH_3Cl$, 593-51-1; $EtNH_3Cl$, 557-66-4.

Literature Cited

(1) Kisza, A.; Tymraklewicz, T.; Zabinska, G. *Pol. J. Chem.* **1981**, *55*, 437.
(2) Kisza, A.; Iwanus, M.; Wlecek, B. *Pol. J. Chem.* **1982**, *56*, 1427.
(3) Kisza, A.; Walczak, B.; Zabinska, G. *Pol. J. Chem.* **1980**, *54*, 2383.
(4) Kisza, A. In *Thermodynamic and Transport Properties of Organic Salts*; Franzosini, P., Sanesi, M., Eds.; Pergamon Press: Oxford, U.K., 1980; Chapter 2.2, pp 243–272.
(5) Gatner, K.; Kisza, A. *Z. Phys. Chem.* (*Leipzig*) **1969**, *241*, 1.
(6) Kisza, A.; Hawranek, J. *Z. Phys. Chem.* (*Leipzig*) **1968**, *237*, 210.
(7) Zabinska, G.; Ferloni, P.; Sanesi, M. *Thermochim. Acta* **1987**, *122*, 87.
(8) Tsau, J.; Gilson, D. F. R. *J. Phys. Chem.* **1968**, *72*, 4082.
(9) Rao, C. N. R.; Ganguly, S.; Ramachandra Swami, H.; Oxton, I. A. *J. Chem. Soc., Faraday Trans. 2* **1981**, *77*, 1825.
(10) Walden, P.; Birr, E. J. *Z. Phys. Chem.* **1932**, *A160*, 161.
(11) Angell, C. A. *J. Non-Cryst. Solids* **1985**, *73*, 1.
(12) Elias, A.; Angell, C. A. *J. Chem. Eng. Data* **1988**, *33*, 1.
(13) Markov, B. F.; Sumina, L. A. *Dokl. Akad. Nauk SSSR* **1956**, *110*, 411.
(14) Markov, B. F.; Sumina, L. A. *Zh. Fiz. Khim.* **1957**, *31*, 1767.
(15) Walden, P. *Z. Phys. Chem.* **1931**, *A157*, 389.
(16) Eyring, H. J. *J. Chem. Phys.* **1936**, *4*, 283.
(17) Angell, C. A. *J. Phys. Chem.* **1964**, *68*, 218.
(18) Angell, C. A. *J. Phys. Chem.* **1964**, *68*, 1917.
(19) Angell, C. A.; Pollard, L. J.; Strauss, W. *J. Chem. Phys.* **1969**, *50*, 2694.
(20) Moynihan, C. T.; Smalley, C. R.; Angell, C. A.; Sare, E. G. *J. Phys. Chem.* **1969**, *73*, 2287.
(21) Easteal, A. J.; Hodge, I. M. *J. Phys. Chem.* **1970**, *74*, 730.
(22) Bloom, H.; Macky, C. J. *Aust. J. Chem.* **1970**, *23*, 1523.
(23) Turnbull, D.; Cohen, M. H. *J. Chem. Phys.* **1961**, *34*, 120 and references therein.
(24) Adam, G.; Gibbs, J. H. *J. Chem. Phys.* **1965**, *43*, 139.
(25) Gawel, W. *Rocz. Chem.* **1975**, *49*, 699.
(26) Gatner, K.; Kisza, A. *Pol. J. Chem.* **1973**, *47*, 1007.
(27) Gatner, K. *Pol. J. Chem.* **1980**, *54*, 1545.

Received for review April 3, 1990. Accepted November 5, 1990. This research has been supported by a 60% fund of Ministero P.I., Rome, Italy. A grant of CNR is gratefully acknowledged by G.Z. The financial support of the 01.15 project is also acknowledged.